



Tactile sensors: A review

Mahmoud Meribout^{a,*}, Natnael Abule Takele^a, Olyad Derege^a, Nidal Rifiki^a, Mohamed El Khalil^a, Varun Tiwari^a, Jing Zhong^b

^a Computer & Information Engineering Department, Khalifa University of Science & Technology, Abu Dhabi, United Arab Emirates

^b School of Instrumentation and Optoelectronic Engineering, Beihang University, China

ARTICLE INFO

Keywords:

Electrical impedance tomography
Piezoresistive sensors
Piezoelectric sensors
Capacitive sensors
Strain measurements

ABSTRACT

Tactile sensing is increasingly attractive in various real-life applications, mainly driven by significant progress in semiconductor, sensing, and material science technologies. Different sensing techniques were suggested for specific design goals, as none of them can simultaneously feature all the properties of human skin: high spatial-temporal resolution and repeatability, ease of stretch and bend, insensitivity to environmental conditions such as electromagnetic Interference (EMI) noise and temperature variations, portability, and determining the intensity of both normal and shear stresses. This has driven researchers to suggest multimodality tactile sensors to enhance their capabilities. However, the sensing techniques focus mainly on five types: resistive, piezoresistive, piezoelectric, capacitance, optical fiber, and visible-light cameras. This paper will reveal the most recent research on tactile sensors, including the sensor, front-end electronics, algorithms, and associated hardware accelerators. It also suggests potential design solutions that can enhance their overall performance. Thus, it can be a valuable tool for researchers and engineers involved in related research activities, as tactile sensing is essential for a wide range of applications, from robotics to medical fields and virtual/augmented reality.

1. Introduction

Tactile sensing, or the ability to feel physical stimulus, can be used in various applications, such as robotic manipulation, prosthetics, surgery, and virtual/augmented reality [1–5]. It facilitates object recognition, grasping, and manipulation, enabling autonomous operations within unstructured environments [6–12]. For instance, in prosthetics, tactile sensors can be used to provide amputees with a sense of touch in their artificial limbs [9,13–15]. This can help them to interact with their environment more safely and effectively. In virtual reality, tactile sensors can create a more immersive user experience [16,17]. For example, a user wearing a virtual reality headset could feel the resistance of a virtual object as they interact with it. As tactile e-skin technologies continue to develop, we can expect to see even more innovative applications of this technology. Several techniques have been employed for tactile sensing to detect the contact location, the pressure, or the strain [18]. This includes capacitive [19], resistive [4], piezoresistive [20], piezoelectric [5,21], triboelectric [5,21], and optical [22] techniques. Capacitive sensing, for instance, measures changes in capacitance to detect deformations and pressure [19,22]. They have the advantage of requiring a simple manufacturing process. However, they may be easily

susceptible to electromagnetic interference (EMI) noises [18]. In addition, they require costly front-end electronics to measure the incremental capacitance variations caused by strains accurately. Optical-based tactile sensing techniques, mainly using fiber bragg grating (FBG), offer high spatial resolution, are scalable, are immune to EMI noise, and yield rapid response time [23–26]. However, the associated hardware is relatively cumbersome and needs a high-power supply [22,25]. Resistive sensing, based on resistive materials, is cost-effective for large-scale deployment [27,28]. However, they solely determine the location of the applied strains, not their intensity. Piezoresistive sensing relies on changes in resistance in response to mechanical pressure on a piezoresistive medium, enabling precise force measurement and localization [22–24]. Compared to optical fiber sensors, capacitive, resistive, and piezoresistive tactile sensors are more accessible to make nowadays and are still flexible enough to accommodate large areas non-invasively. Thus, they offer high potential, especially since their associated front-end electronics are simpler [24,29]. Taking advantage of the significant progress of video cameras and associated hardware accelerators, visual-based tactile sensors that use markers, densely distributed on a flexible material, have recently emerged [30,31]. Some are commercially available to yield 1 mm sensitivity in all three directions. Still,

* Corresponding author.

E-mail address: mahmoud.meribout@ku.ac.ae (M. Meribout).

they are limited to covering relatively small areas (i.e., less than 2 cm² area) and are not easily scalable. The associated algorithms of these sensors can be either ET-based to reconstruct the two-dimensional (2D) strain distribution [32] or non-ET-based using some analytical circuit equations, which may be augmented with the use of artificial neural network (ANN) or convolutional neural network (CNN) algorithms. ET-based algorithms usually yield richer information using fewer electrodes; however, as of now, they are limited to only a few tens of pixels in the image space, and they usually generate relatively poor spatial resolution images with poor contrast. Their challenge is to deal with an ill-posed nonlinear mathematical problem, lowering the accuracy of the reconstructed image, especially with the increase in the number of strain points [35]. The other challenge comes from the conductivity or dielectric constant distribution of different materials composing the sensor element, which is usually not uniform, making the sensor's mathematical modeling challenging and not generalized. Another challenge is the crosstalk problem caused by the dense electrical wiring to connect the electrodes. Several researchers have tackled these issues from either the hardware (e.g., using multimodality imaging using additional ultrasonic sensors [36]) or from the algorithmic points of view using signal processing, machine learning [29], and look-up tables [37] methods.

This review paper will address recent advancements in improving the spatial resolution, sensitivity, and scalability of various types of tactile sensors. This includes the hardware (i.e., the front-end analog electronics and the digital hardware accelerator) and algorithm aspects where AI has effectively contributed to its advancement. Several other review papers on tactile sensing were recently published. Table 1 summarizes some of them. For instance, in [33], the measurement errors induced from resistive sensor arrays due to crosstalk interference noise between nearby tracks were comprehensively reviewed. It was concluded that the voltage feedback non-scanned-sampling-electrode (VF-NSSE) technique is the most effective for mitigating the effect of the crosstalk. More recently, in [38], different methods to fabricate tactile sensors were listed. They mentioned that textile-based materials are more promising than polymer counterparts regarding breathability, ease of bentness, and lightness. They also revealed the pending challenges of tactile sensors, such as crosstalk between adjacent cells and eventual mechanical deformation of neighboring cells and methods to mitigate them. These papers were limited to addressing the issues faced by various resistive sensor elements. This review paper covers a broader range of tactile sensors, including all the hardware parts and the associated algorithms. This makes it a valuable resource for researchers working in this area. Other review papers listed in Table 1 focused on AI algorithms used for tactile sensing [89–93].

The paper is organized as follows: A review of tactile sensors and associated front-end electronics is illustrated in Section 2. This includes resistive, piezoresistive, capacitive, and optical sensors. The section provides a detailed discussion involving other new technologies, such as

Table 1
List of some recent reviewer papers on tactile sensing.

Number	Reference	Title	Year
1	[33]	Measurement errors in the scanning of resistive sensor arrays	2010
2	[38]	Recent progress in high-resolution tactile sensor array: From sensor fabrication to advanced applications	2023
3	[89]	Learning-based robotic grasping: A review	2023
4	[90]	Deep Learning Approaches to Grasp Synthesis: A Review	2023
5	[79]	A review of robotic grasp detection technology	2023
6	[92]	Robot learning towards smart robotic manufacturing: A review	2022
	[93]	Vision-based robotic grasping from object localization, object pose estimation to grasp estimation for parallel grippers: a review	2021

compact visible cameras and multimodality sensing techniques. Sensor 3 describes various AI and non-AI algorithms used for tactile sensing. The paper ends with a Conclusion section summarizing the paper's findings and the prospects of tactile sensing.

2. Tactile sensors and associated front-end electronics

Fig. 1 shows a typical hardware block diagram of a capacitive, resistive, or piezoresistive-based tactile sensor. Depending on the electrical properties to explore when applying a strain (e.g., conductivity or capacitive changes), the sensor's excitation can be done using an electrical current or voltage source. The current/voltage excitation is done in a time multiplexer manner to scan the whole sensor and determine the strain distribution in real time, which includes, in some cases, their respective intensity. A controller based on a Field Programmable Gate Array (FPGA) and GPU is used to schedule the scanning process and collect the corresponding data. The measurement algorithm is then performed for 2D image reconstruction of the applied strain. This usually requires high computation power where edge FPGA or GPU can be adequate. The sensor can comprise a stack of several conducting and non-conducting materials, which can be made of nanocomposite compounds comprising different kinds of nanoparticles. They can also be composed of ionic liquid, which flows along miniaturized conduits according to certain strain distributions. One challenge of composite materials is the irregular conductivity distribution because of the random arrangement of nano-particles and fibers.

This makes the design of the associated front-end electronics and measurement algorithm challenging. Thus, almost every tactile skin requires its own training and calibration procedure. Ionic liquid solves this issue but may be prone to leakage and feature low SNR (signal-to-noise ratio), leaving more floor-to-composite materials [39,58]. A third alternative is to use a stack of nonconductive materials (e.g., flexible printed circuit boards, PCB), within which at least two layers comprising parallel conductive tracks are used [40–42]. FBG-based tactile sensors have a similar design, as shown in Fig. 1, in that the current/voltage source is substituted by a light sensor enclosed within an optical integrator. This latest also comprises a photodetector that receives a narrowband light spectrum to determine eventual strains based on the phase difference of the associated wavelength. In this case, one flexible layer is enough, and its electrical properties are unimportant as the optical fiber only carries the signal.

2.1. Resistive tactile sensors

2.1.1. Principle of operation

Usually, resistive tactile sensors consist of at least two layers of flexible, highly electric-conductive mediums separated by a highly porous and much less-conductive layer, such as foam. An array of electrodes is usually placed at the bottom conductive layer, typically at its border, to sense any voltage that originates from the top layer when it is exposed to a strain (Fig. 1). A DC current source is usually applied to the top layer as a short circuit may be induced when the bottom and lower layers are in contact. At rest, when no strain is applied, the top and bottom layers are not connected, and no voltage can be sensed across the electrodes. Thus, these sensors are not designed to determine the strain intensity but only their location by exploring the resistance changes induced by the application of the strain. These sensors are fabricated so that the electric resistance changes with the applied strain, not to be accurate but to yield at least two distinguishable levels of conductivities corresponding to the ON-OFF strain. Signal conditioning usually consists of an amplifier and an ADC module that lets an embedded processor process the collected data. Thus, one of the advantages of this sensor in tactile sensing is its simplicity and low cost; however, as discussed in section A.3, a series of challenges still need to be addressed to have it adequate for real-life applications.

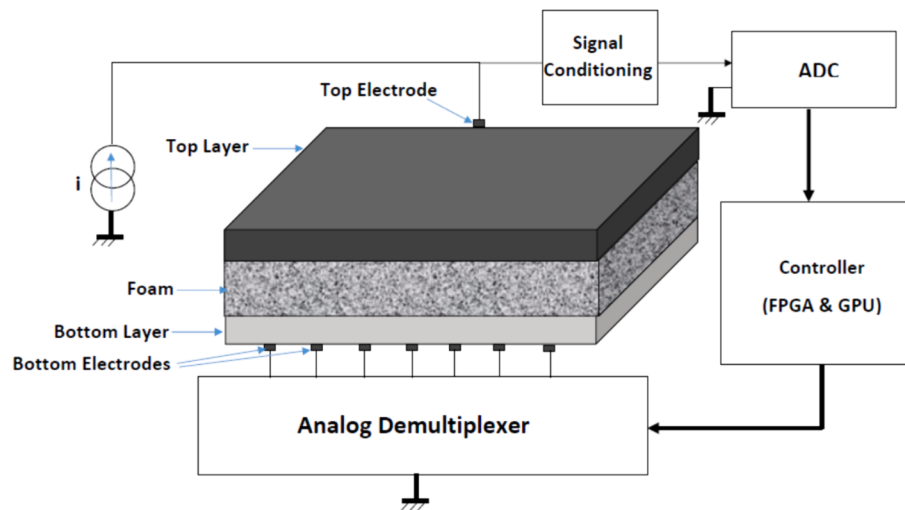


Fig. 1. Typical hardware block diagram of a tactile sensor.

2.1.2. State of the art works

Various design changes were suggested for resistive-based tactile sensors to improve some specifications, but the principle, as mentioned in Section A.1 above, remains the same. For instance, in one of the recent works, a $20 \times 20 \text{ cm}^2$ tactile sensor that explores the contact resistance changes between a stretchable base conductivity layer and highly conductive fabric-independent 20×20 patches was suggested [29] (Fig. 2). The base conductivity layer is manually created in-house by applying carbon black spray to the target area, allowing for the formation of the layer on any desired surface of the body under investigation. Sixteen electrodes were incorporated into this layer by evenly screwing them onto its edges and adding another one at its center by applying silver paste.

The front-end electronics are designed so that an electrical current is injected into the electrode at the center towards one of the peripheral electrodes. Voltage measurements are then taken sequentially between the central electrode and the other peripheral electrodes using an analog multiplexer. Thus, with 16 peripheral electrodes, 256 measurements are taken. Subsequently, the collected data is processed using an Electrical Impedance Tomography (EIT)-based ANN algorithm to generate the 2D image corresponding to the applied strain distribution. Unlike the ERT-based sensor, this sensor explores the measured voltage amplitude and the phase difference between the current and voltage, yielding further information on eventual strain distribution. According to the authors, the system could yield accurate 2D image reconstruction, overcoming the spatial limitation of the EIT algorithm, especially at the center of the image, by using the central electrode. In addition, compared to piezoresistive sensors, the system features a more uniform distribution of the electrical conductivity of both the top and bottom layers. The data processing hardware consists of an FPGA board for current channel

selection and data acquisition, and all processing is done on a PC using the Labview software [35]. This may hinder its real-time performance, as about 64 ms was required to perform one 2D image reconstruction. Furthermore, the spatial resolution was limited to 9×9 locations using a circular tip of 2 cm in diameter and a relatively high pressure of 23 N, which may not be adequate for robotic applications. In addition, only four-strain points were tested to yield humble results where the mean square localization error (MSE) was $4.88 \pm 1.63 \text{ mm}$, $6.62 \pm 2.98 \text{ mm}$, and $8.22 \pm 4.29 \text{ mm}$ using the suggested EIT-NN, the iterative Gauss-Newton (GN) and one-step GN algorithms, respectively. This is a common feature of resistive-based tactile sensors where large area coverage using fewer electrodes compromises the spatial resolution. Several other resistive tactile sensors mainly use similar designs with incremental variations on the number of layers used, the pattern of the conductive tracks, the electrode placements, and the reconstruction algorithms. Another design style is to consider parallel conductive tracks placed in two isolating and flexible PCB layers. The two layers are separated with a highly porous medium and placed so that the tracks of the two layers are perpendicular [33]. For instance, in [82], a conductive polymer composite (CPC) material sandwiched between two sets of 32 orthogonal electrodes, made of smoothed stainless-steel electrodes, was used (Fig. 3). The system was designed to target real-time applications where 100 frames/second throughput could be achieved using ARM Cortex M7 microcontroller which controls the channel selection and the ADC conversion sequences. Twenty-six objects were trained using a customized CNN model to achieve an accuracy of 77.84 % with a maximal power consumption of 505 mW. This work is rare and requires a complete design and build of an embedded real-time tactile sensor. This category of sensors is simple and easy to fabricate but has the disadvantage of exposure to high EMI noise, which requires a special

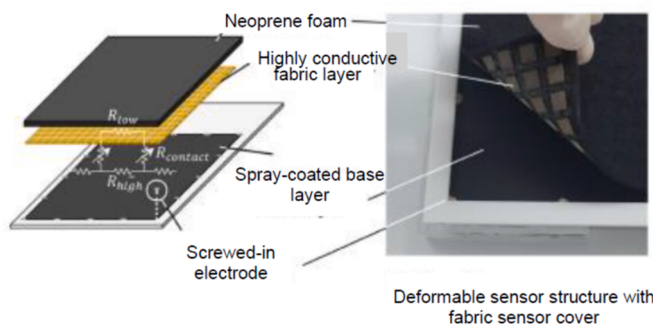


Fig. 2. Resistive tactile sensor as suggested in [29].

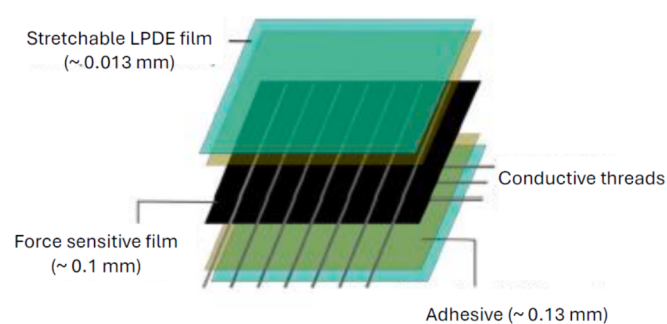


Fig. 3. Resistive tactile sensor as suggested in [82].

shielding design [35]. Indeed, the EMI noise is even more pronounced for capacitance and piezoelectric sensors since capacitance values of nF order and electric charges of pC order, respectively, are sought to be measured.

One common issue with resistive sensors is the effect of material conductivity on their sensitivity and the range of forces they can handle. This was tackled recently in [96], where the authors investigated the sensor conductivity effect on the stress range that can be supported. The results, supported by experimental work on tangible input interfaces, soft grippers, and flexible-tough displays, revealed that a conductivity of 0.2 S/m can detect forces of up to several newtons.

2.1.3. Features of resistive-based tactile sensors

As mentioned, these sensors are relatively simple to design, cheap, and adequate to cover large e-skin areas. Also, using the EIT technique, fewer electrodes can yield an excellent spatial resolution. One noticeable difference between EIT systems for tactile sensing and those for monitoring conductive fluids is that the applied current is DC, not AC. This helps to exhibit the data acquisition time, as waiting for an entire clock cycle to generate a single voltage reading is unnecessary. Unlike conductive fluids, conductive fabrics are not prone to polarization, which may accelerate the corrosion process of the electrodes. This allows the use of DC current excitation, which is more straightforward to design. However, they can only detect a few contacts and are sensitive to temperature variations. Redesigning the sensor using regular conductive track patterns rather than a single-piece conductive layer can overcome these challenges. Also, these sensors yield low spatial resolution, especially in areas away from the electrodes, as they adopt a linearized inverse model. However, this may also increase the EMI noise, which would require special shielding of the system. In addition, the conductivity of the bottom and top conductive layers is not uniform, which violates the assumption of the EIT algorithms that the conductivity of the background medium shall be uniform. This has caused these sensors to feature relatively weak spatial resolution, which may need to be improved in robotic applications [29]. Nevertheless, other nanoparticle injection sensors (e.g., piezoresistive and capacitive sensors) also struggle to yield good repeatability because of their random distribution and inconsistency in the manufacturing process. Thus, material selection remains a hot topic in tactile sensing. The use of ionic liquid was suggested to overcome these issues. However, the associated sensors present leakage risks and may not be suitable for outdoor applications where uncontrolled temperature may lead to evaporation or solidification of the liquid. Resistive-based tactile sensors also consume relatively large power compared to piezoelectric and capacitive sensors since the values of load resistances are relatively low.

2.2. Piezoresistive-based tactile Sensors

2.2.1. Principle of operation

Unlike resistive tactile sensors used to localize the points of strains only, piezoresistive sensors are used to determine both the location and intensity of the strains. This can be useful in several applications as it yields a sensing behavior closer to human beings. The application of a strain γ on a material of initial resistance at unrest, R , would cause a change of resistance ΔR according to the equation:

$$\frac{\Delta R}{R} = (1 + 2\sigma + \pi E)\gamma \quad (1)$$

where σ is the Poisson's ratio of the material and π the piezo-resistivity coefficient, and E the Young modulus. Thus, piezoresistive-based tactile sensors have a structure similar to resistive counterparts, only that the middle flexible layer is less porous and has good piezoresistive properties.

2.2.2. State of the art works

[Fig. 4](#) shows one very recent electrical resistance tomography (ERT) $54 \times 54 \text{ cm}^2$ tactile sensor that uses this concept [49]. Two textile conductive sensors separated by a porous conductive foam were used. The top layer of this structure functions as a highly conductive sheet, serving as a large electrode. Conversely, the bottom layer comprises a high-resistance fabric with 28 electrodes distributed across its surface. These electrodes are intricately sewn to the high-resistance fabric using conductive thread and serve the purpose of measuring the overall voltage across the conductive foam.

As per the study, an intermediate layer of an Electrostatic Discharge (ESD) foam separates the two sets of electrodes. Similarly to EIT-based tactile sensors, a DC electric current to the top electrode to subsequently measure the voltage at each of the distributed electrodes on the bottom layer sequentially [6,32,33]. The conductive foam's porous structure introduces substantial resistance between the highly conductive top layer and the distributed electrodes on the bottom layer, which is reduced proportionally to the applied force [32]. The acquired voltage measurements across the conductive foam, are then captured and subjected to processing using a purpose-built ERT-based ANN. As discussed further in Section III, this algorithm is specifically designed to process and analyze tactile data from the input layer to the output layer for 2D image reconstruction of the touch distribution. 784 voltage readings are processed within 30 ms, achieving real-time performance. Nevertheless, placing the electrodes in the middle of the lower conductive fabric could affect the system's flexibility and engender higher cross-talk noise. Consequently, the average error was 77.4 mm, representing 17.2 % of the sensor width, while the force error was around 13 %. Also, the system was tested to determine the location and strain of up to 7 contact points only but without showing their associated strains. Another recent study suggested a fabric-based sensor yielding 54 image pixels using four layers of different non-conductive and conductive fabrics ([Fig. 5](#)) [34].

The sensor utilized a knitted fabric with piezoresistive and stretchable properties comprising 75 % nylon and 28 % spandex. To enable conductivity, this fabric was coated with a conductive polymer. The piezoresistive fabric was positioned between two highly conductive materials, and the resistance changes at the two layers were monitored when pressure was applied to the composite structure. This design will only be able to detect if a strain pressure has been applied to the electronic skin, not its location. As a result, the electronic skin was cut into small-sized patches by etching it with Ferric Chloride (FeCl₃) to create distinct regions of sense. A set of 54 patches was then made to yield 54 electrodes for current injection and voltage measurement. A fourth nonconductive flexible layer protects the sensor against eventual human sweat, which may cause moisture and thus change the sensor's electrical conductivity characteristics. The model exhibited good signal repeatability in the low, medium pressure range, 0–50 kPa when a non-conductive spacer layer of 0.23 mm thickness is placed between the one conductive layer and the middle layer. Thus, the sensor is appropriate for robotic and bioengineering applications that require high sensitivity to minor applied strains. Among the few experiments done on the sensor, the weak repeatability of the sensor in responding to a constant strain of 10 kPa, where a voltage variation of up to 4 % was observed. This may be due to the foam's relatively random resistivity behavior and the crosstalk interference noise, as several wires are connected to nearby internal electrodes. This design could have further been enhanced by carefully studying the tactile signatures of the human hand and generating an associated refined dataset [35]. However, it constitutes a substantial improvement over other similar works [36] where the tactile sensor, in the shape of the glove, could not be removed from the hand without destroying the sensor and hence not reusable. No front-end electronics or hardware accelerators were used, and the setup was limited to a variable voltage source and PC equipped with a 16-bit data acquisition card to capture the voltage across pairs of electrodes, which were selected manually. Another approach presented a

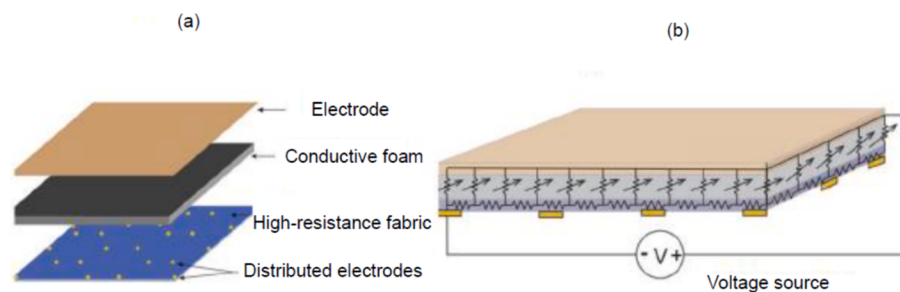


Fig. 4. (a) The layered structure of the ERT tactile sensor (b) A schematic of the conductivity model. [49].

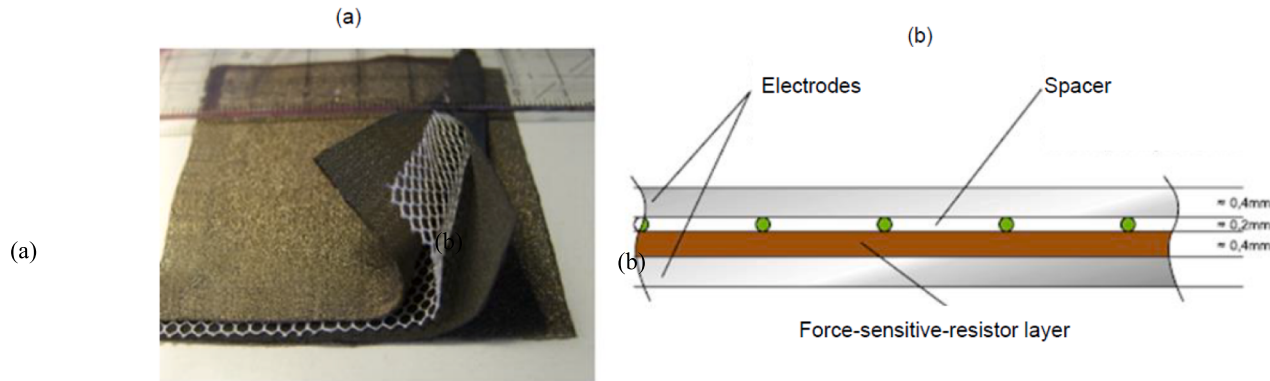


Fig. 5. Piezoresistive tactile sensor as suggested in [34]: (a)- Photography of the tactile sensor and (b)- schematic of the sensor.

meticulously designed piezoresistive $5.6 \times 5.6 \text{ cm}^2$ tactile sensor array tailored explicitly for a humanoid robot hand [37,38]. The system's contribution is automatically recognizing 13 objects of different shapes and weights based on tactile sensing with an accuracy of 92.73 %. The sensor, which yields a 16×16 pixels image, is structured into five layers. The bottom layer acted as the substrate, the base, and the insulator. The top layer comprises arrays of electrodes functioning as a conductor. The third layer comprised the conductive polymer, which acted as a piezoresistive material with variable resistance based on applied forces. The topmost layer was an elastic overlay, functioning as both a receptor and a force transmitter, utilizing the conductive polymer. Following this approach, a humanoid robot hand was built to perform grasping and use the Deep CNN (DCNN) model to perform object recognition from a tactile input. The implementation of various DCNN models is reviewed in section 4. The front-end electronics of the system are based on an Arduino board (Mega2560 version), and the data processing and DCNN were implemented on a PC. The fact that each pixel element is connected to a wire makes the scalability of the device to handle higher image resolutions very challenging. With the significant progress of edge hardware accelerators for object recognition using visible light or infrared cameras, camera-based tactile sensing is expected to be a better alternative.

Among the rare works that used only one flexible material, one can cite the hydrogel sensor which was in-house fabricated by homogeneously mixing hydrogel, acrymelid, acrylic acid, and methylenebisacrylamide with water and drop it into a $200 \times 200 \text{ mm}^2$ ecoflex substrate [39]. Sixteen electrodes were then placed on the boundary of the sensor, and an ET-CNN algorithm was used. An ADC5940 signal generator (0 to 200 kHz sinusoidal signal) chip and a 16 to 1 multiplexer, ADG706, were used together with an STM32 microcontroller to control the data acquisition sequences. Furthermore, a 4-wire impedance analyzer was used to determine the impedance changes. Image reconstruction was done using a PC. Experimental work was done on only one single strain contact for different strain intensities; however, this concept is worth exploring further as the fabrication process is

simple and quick. Recently, a neuro-inspired artificial peripheral nervous system for scalable electronic skins using resistive elements was suggested [40]. The sensor mimics the human sense of touch, consisting of many sensors, namely mechanoreceptors, independently connected to the processor. The processor captures the spatial-temporal spikes that may be induced by the individual mechanoreceptors using a summer circuit. It has the advantage of yielding a high-speed acquisition time as it is event-driven and does not use the time-multiplexing technique to measure the sensing signals of individual sensors, making it scalable enough to handle large areas. Furthermore, the suggested e-skin is more fault tolerant to the traditional matrix resistive sensors since a failure on one conductive trace or mechanoreceptor does not affect the others. The authors used 254 receptors to validate their approach, each having its unique conductive trace. The time delay between adjacent traces was set to 60 ns to yield an impressive 1 mm resolution; however, the device is still in the prototyping stage.

2.2.3. Features of piezoresistive-based tactile sensors

Piezoresistive sensors have been widely used in tactile sensing because of their high sensitivity, good spatial resolution, and well-mature technique. In addition, they are cost-effective and relatively easy to implement. They are less noise-prone than capacitive-based tactile sensors, and unlike piezoelectric sensors, they can handle static and dynamic pressure. This makes piezoresistive sensors suitable for grasping applications and object recognition [41]. They typically provide contour information of objects and are usually combined with other sensors, such as piezoelectric sensors, to provide inner pressure information. Similarly to resistive sensors, piezoresistive sensors are sensitive to temperature variations and can hardly yield a uniform piezoresistive property along the whole area.

2.3. Piezoelectric-based tactile sensors

2.3.1. Principle of operation

These sensors work based on the piezoelectric effect that when the

sensor is exposed to an external force, F , electrical charges, Q , will be generated proportionally according to the following equation:

$$Q = dxF \quad (2)$$

Where d is the charge sensitivity of the piezoelectric element. For tactile applications, they are usually based on polyvinylidene fluoride (PVDF) material as it is flexible to take various shapes of the target objects. A highly sensitive charge amplifier is required to convert the charges to an output voltage, making its signal conditioning more complex than the one for resistive and piezoresistive sensors. They can be self-powered to detect transient strains as their sensitivity in low frequency is null.

2.3.2. State of the art works

Among the very recent sensors, one can mention the one disclosed in [42] where a spatial resolution of 200 μm , comparable to a human fingerprint, could be achieved using a 12×16 polyvinylidene fluoride (PVDF)-based piezoelectric sensor array fabricated with 0.18 CMOS technology (Fig. 6). Experimental results reveal that using an on-chip spiking neural network (SNN), an accuracy of 99.2 % could be achieved using only 256 neurons, with a spike encoding resolution of 3–5 bits. The chip, which consumes only a maximum power of 5 mW, is meant to mimic human fingerprints.

Similar sensors were also suggested in [42–45] to yield very high spatial resolution (sub-mm) at low power consumption, making them typically used at the fingertips of robots.

2.3.3. Features of piezoelectric-based tactile sensors

These sensors do not require a power supply source to operate and can be integrated with high density using a CMOS process to achieve high spatial resolution. In addition, their impulse output makes them suitable for accommodating spike neural networks seamlessly onto a single neuromorphic chip. In addition, they are stable and less prone to electromagnetic interference noises compared to resistive and piezoresistive sensors. They were also demonstrated to detect slide movements on the target object, which can benefit many applications [46]. However, their drawback is the relatively complex signal condition circuitry requiring a charge amplifier and high precision preamplifier for each

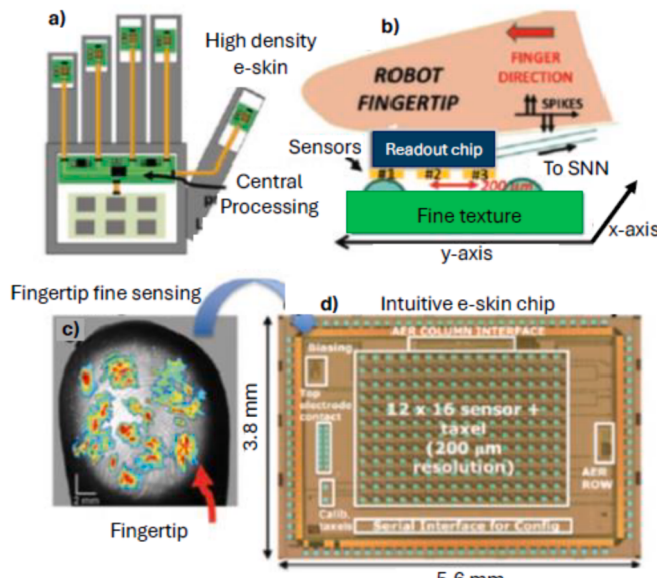


Fig. 6. (a) Equipping a robotic hand with a combination of large-area eskins in the palm and high-spatial-resolution e-skin on the fingertips allows the classification of b) macro and micro tactile features. (c) The receptor density and complex receptive fields in human fingertips are mimicked in the presented d) INTUITIVE e-skin sensing chip [42].

taxel, which increases their cost. However, compared to the capacitance sensor, the signal conditioning circuitry is much less complex for the same spatial resolution. It can also yield lower latency if event-driven data acquisition is used, which cannot be used with capacitance-based tactile sensors. These sensors are also sensitive to temperature variations and feature a narrow bandwidth, which limits their suitability to accommodate dynamic forces at high frequencies, which is the case for grasping tasks.

2.4. Capacitive-based tactile sensors

2.4.1. Principle of operation

These sensors consist of at least one compressible dielectric layer (e.g., microstructured rubber layers, [47] polymer transistors [38], self-healing composites [48] and orderly array inorganic nanowires, [49]) inserted between electrodes which are sequentially excited by a voltage source. This allows us to determine the capacitive value, C , at different positions of the sensor, which depends on the applied strain according to the equation:

$$C = \epsilon_0 \epsilon_r \frac{A}{d} \quad (3)$$

where d is the variable distance between the two electrodes being affected by the strain, A is the area of the two opposite armatures, which is constant, and ϵ_r is the relative constant dielectric value of the dielectric layer. These tactile sensors are more stretchable than piezoresistive sensors, typically designed on stiff substrates. In addition, they are less sensitive to temperature variations. Thus, these sensors, which can be either area-variable (changing A in Eq. (2)) or electrode-spacing-variable changing d in Eq. (2), have attracted the interest of many researchers and companies. However, electrode-spacing variable tactile sensors are more widely used since they feature a more extensive pressure range than the area-variable type and are less fragile despite being less sensitive.

2.4.2. State of the art works

These sensors typically consist of $n \times m$ pair plates separated by a dielectric material and connected to a $(n \times m)$: 1 multiplexer for tactile sensing. This latter is fed to a highly sensitive capacitance sensor, usually a voltage-to-capacitance converter, the accuracy of which requires a long-time delay, causing a slow acquisition time compared to the other sensors. In [50], a simple manufacturing technique was suggested to create a 7×7 capacitive-based flexible and wearable tactile sensor (Fig. 7).

The cost-effective multifunctional sensor array features compassionate touch, pressure, and strain detections statically and dynamically. It consists of dielectric layers and polyethylene terephthalate (PET)-based silver (Ag) serpentine-shaped electrodes, creating a capacitive sensor whose detection limit is 6 Pa. Three sensing modes were demonstrated to map contact, pressure, and strain distributions, respectively, with good repeatability and sensitivity of the sensor caused by a single water droplet. However, the sensor's response time, 100 ms, was relatively long for real-time tactile sensing. Furthermore, the front-end electronics are not revealed in the paper, and the sensor accuracy is expected to be complex to handle readings in the ff order. This range can be predicted considering the area of the armature plates. In conclusion,

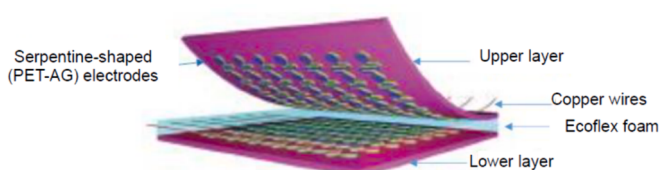


Fig. 7. Capacitive-tactile sensor as suggested in [50].

this work is far from getting mature, and further efforts are required in the electronics and data processing parts. Decoupling the force direction with capacitive tactile sensors is still tricky since no clear theory explaining the relationship between input force and output signal and the process behind force and deformation still needs to be determined. A recent 2×2 capacitive flexible tactile sensor that uses a dielectric layer with a microcylindrical structure to sense external loads to address this issue was suggested in [51]. The strain capacity of the dielectric layer is increased by its micro-cylindrical structure, which also improves the sensor's performance. Examining the sensor coupling, they also provide a decoupling model based on the deformation mechanism. Additionally, they integrate the sensor into a soft rehabilitation glove and a soft gripper to validate its use in tangential detection and object gripping. The sensor exhibited a low hysteresis of 3.5 %, a normal sensitivity of 0.33 N^{-1} , and a tangential sensitivity of 0.091 N^{-1} . Forces ranging from 0.5 to 4 N were assessed. However, electronics were not built as the assessment was done using only a commercially available LCR meter (LCR-821, GWINSTEK) to measure the capacitance at 100 kHz and 1 V excitation. A positive note is that the sensor was successfully tested for two applications: non-destructive fruit gripping and rehabilitation gloves. In [47], a $9 \times 9 \text{ mm}^2$ triaxial flexible single-pixel tactile sensor with a bump-force conducting framework made of four capacitors was created and assembled (Fig. 8). To mitigate the inertial disturbance, a bump-force conducting structure was added, allowing the force acting on the tactile sensor to be distributed evenly. The inertial disturbance was also quantified and analyzed, and a compensation method that uses the acceleration signal as a reference was suggested. As a result, a sensitivity in the order of micronewton was claimed to be achieved.

This work is one of the rare ones that has used a dedicated front-end electronics circuit that consists of a single chip 24-bit capacitance to digital converter (CDC), AD7746 (from Analog Devices). The IC has a built-in temperature compensation circuitry and yields an impressive accuracy of $\pm 4\text{fF}$ for a capacitance range of up to 4 pF. However, the sensor has a humble response time of 100 ms, which makes its usage to handle hundreds of capacitances required in a reasonable-size tactile sensor just impractical. Special care must also be taken against EMI noise, which can easily exceed the fF range. Recent work has suggested eight capacitive sensing elements, such as tactile sensors targeting a robotic finger, to measure the strain intensity ranging from 1 to 16 N (Fig. 9) [52]. The sensor has an update rate of 400 Hz and a resolution of 50 fF. The measurement unit determines the In-phase quadrature (IQ) variable, providing the signals' amplitude and phase under an 81 kHz excitation.

In summary, while capacitance-based tactile sensors have the advantage of being more stretchable and less temperature dependent than resistive and piezoresistive sensors, they face the issues of dealing with very low capacitance values, which require a complex design of the front-end electronics, undoubtedly challenging for making compact and easily portable, especially if real-time performance and scalability are sought.

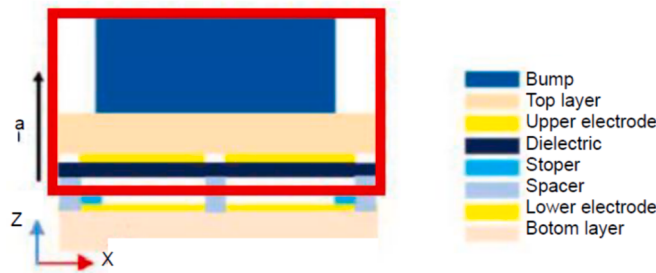


Fig. 8. Schematic of the tri-axis tactile sensor suggested in [51].

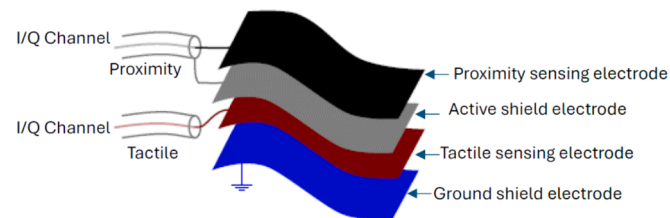


Fig. 9. Capacitive-based tactile sensor as suggested in [52].

2.4.3. Features of capacitance tactile sensors

Capacitance-based tactile sensors have the advantages of being more stretchable than piezoresistive sensors and being less sensitive to temperature variations compared to resistive and piezoresistive sensors. They can also yield high spatial resolution and high force sensitivity in the sub-mm sub-N ranges, respectively. Also, up-to-date, they are the only sensors that can measure lateral strains or shear forces in addition to the regular forces by changing the variable, A, in Equation (2) [29].

However, these types of sensors require advanced electronics to read fF capacitance values in the case of miniaturized e-skin. The accuracy usually increases with increasing latency to allow full charge-discharge of the capacitances. Also, they are sensitive to humidity and can't work near metallic parts. Therefore, when using capacitive tactile sensors in robotics or biomedical tasks, it is essential to consider the material of the surrounding objects carefully.

2.5. Optical tactile sensors

2.5.1. Principle of operation

Optical sensors for tactile sensing are usually based on the FBG principle, which consists of an optical fiber tightly placed on the target object. A source of wide-spectrum light is emitted on one side of the fiber, and a detector, placed on the same side, receives a sequence of narrow-band lights. The wavelength shifts of the received lights, $\Delta\lambda_B$, about the expected Bragg wavelength, λ_B , indicate the intensity of the stress, $\Delta\epsilon$, and temperature, ΔT , at different predefined locations of the fiber (Fig. 10) according to the following equation [31]:

$$\frac{\Delta\lambda_B}{\lambda_B} = \{k_e \Delta\epsilon\} + \{k_T \Delta T\} \quad (4)$$

where k_e is the total strain, and k_T is the total temperature sensitivity factor of the FBG sensor. This equation of two unknowns requires deploying a second unstressed optical fiber to determine the second term ΔT . However, most existing FBG-based tactile sensors neglect temperature variations and use only one fiber, making them prone to significant errors in unconstrained environments.

These sensors are compact (in terms of wiring), electromagnetically immune, multiplexable, and capable of distributed sensing. In addition, the fabrication of the sensing element is more straightforward as its conductivity and dielectric constant values do not matter. They are inspired by nerve fibers in the human skin, which capture mechanical stimulation and convert them into receptor potentials. Hence, they are emerging quickly as a viable alternative to tactile sensors.

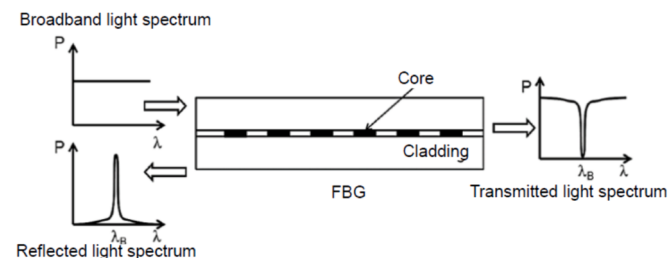


Fig. 10. Principle of FBG sensors.

2.5.2. State of the art works

In [53], an $8 \times 8 \text{ mm}^2$ skin-like optical fiber tactile (SOFT) sensor driven by AI is suggested to detect a single contact point on a 2×3 sensor array (Fig. 11). The sensor has multipurpose touch interface properties, such as tensile strain, tactile amplitude, and position. With a stretchability exceeding 20 %, the SOFT sensor's skin-like three-layer laminate construction contains four fiber Bragg gratings (FBGs) that form a flexible tactile sensing array. With a force range of 0–3.5 N, the recognition accuracy for contact position is 92.41 %, and the error is less than 4.2 %. Nevertheless, the authors did use a cumbersome FBG integrator and did not mention how they tackled the typical issue of temperature compensation required for FBG sensors. In the experiments, the authors tested only one single contact. Similarly, in [25], a 20 mm diameter optical contact force sensor for tactile sensing based on specklegram detection was proposed and verified for a strain ranging from 0 to 23 N. Two of the structures were chosen, one based on the few modes fiber (FMF) and the other one on multimode fiber (MMF) concatenation. The sensor measured the strain intensity, not its location, and the sensitivity was less than 0.087 N^{-1} with a standard deviation of 0.0219. However, no accuracy assessment was conducted on the sensor.

In more recent work, a 3D-printed FBG tactile sensor targeting a nursing robot was designed and built [31]. The sensor, which consists of 4 sensing units, separated by 4 mm, exhibits an impressive sensitivity of 225.038/N and a response time to step excitation of 2 ms, with 32.93 dB SNR. The percentage error was less than 4.4 %, and the author claimed that the sensor can discriminate between male and female pulse waveforms before and after exercise. Likewise, a more recent modular FBG-based tactile sensor was suggested in [54] to yield a sensitivity of 1.45 N and a spatial resolution of 1.91 mm. FBG sensors have recently emerged to be deployed for robot-assisted minimally invasive surgery (RMIS) applications, and they are biocompatible, unlike resistive and capacitive devices. In addition, they are more compact (except for the integrator part), not toxic, and corrosion-resistant. In [54], another recent six-axis FPG-based temperature-compensated tactile sensor for measuring the force/moment was suggested. The sensor was meant to assist endoscopy visual feedback to characterize inner tissue (e.g., identification of buried hard-inclusion and blood vessels). This outperforms the piezoelectric-based tactile device suggested in [55], which can identify the inner wall shape in a blood vessel but in only one axis force instead of six. It also outperforms another six-axis capacitance-based tactile sensor [56] meant for the same endoscopy application. Still, the device is not biocompatible and does not operate with a Magnetic Resonance Imaging (MRI) device placed in the same probe. A dedicated BPNN-based non-linear decoupling algorithm was used to diagnose and modify the sensor's fault response under different FBG fracture situations. The system was successfully tested on phantom blood vessels ($180 \times 100 \text{ mm}^2$)—another recent FBG-based tactile

sensor targeting nursing applications (i.e., massage of patients) [57]. The sensor comprises four sensing elements separated by a 4 mm distance and placed on a 3D-printed resin-made skin. Hence, many FBG-tactile sensors were suggested, but none is commercially available due to their high cost and relatively low spatial resolution.

2.5.3. Feature of optical-based tactile sensors

Optical sensors are the only sensors with the advantage of not being sensitive to EMI noise, which constitutes an obstacle to increasing simultaneously the resolution and the size of the tactile sensors. However, their sensitivity to stress is lower and decreases with the distance separating the two sensing points [58]. In addition, they can't cope with bending deformation and require cumbersome FBG integrators, which are not easily portable. Another challenge not addressed in the literature is the requirement to measure temperature variations at every grating point, which is practically hard to deploy. These attributes make FBG sensors for tactile applications more suitable for touch sensing than stress and pressure sensing and are more adequate for relatively high values of strains (i.e., more than 1 N strain).

2.6. Magnetic tactile sensors

2.6.1. Principle of operation

Magnetic sensors were also used for tactile sensing, which features various advantages. They use a pair of magnetic field generators and magnetic sensor arrays, usually hall-effect or giant magnetoresistance (GMT) sensors, that detect a strain proportionally to the received magnetic field. Initially, permanent magnets embedded in soft materials (e.g., silicone rubber) were used [59,60], which, however, were substituted by magnetic fillers since they are more flexible and occupy less volume [61].

2.6.2. State of the art works

Several magnetic-based tactile sensors were suggested in the literature. For instance, in [62], a single Hall-effect sensor was used for tactile sensing on a finger to detect forces from 0.01 to 3 N. Similarly, in [63], three Hall effect sensors were used to yield a three-dimensional normal and shear force measurement in 0–4 N and 0–1 N, respectively. In addition, GMT sensors were used, featuring high sensitivity to detect even small magnitude forces (down to 3 mN in [64]). In [64], a GMT-based magnetic tactile array sensor comprising 4×2 elements was designed on a single Si chip to target fingertip application and yield a measurement range from 0.1 to 5 N. More recently, in [66], a GMT sensor, a flexible magnetic film, and four connected columns were used to detect normal and shear forces. The sensor (Fig. 12) features pressure and shear sensitivities of 0.087 kPa and 0.2 N, respectively, within a range of [0 to 5 kPa] and [0 to 0.05 N], respectively.

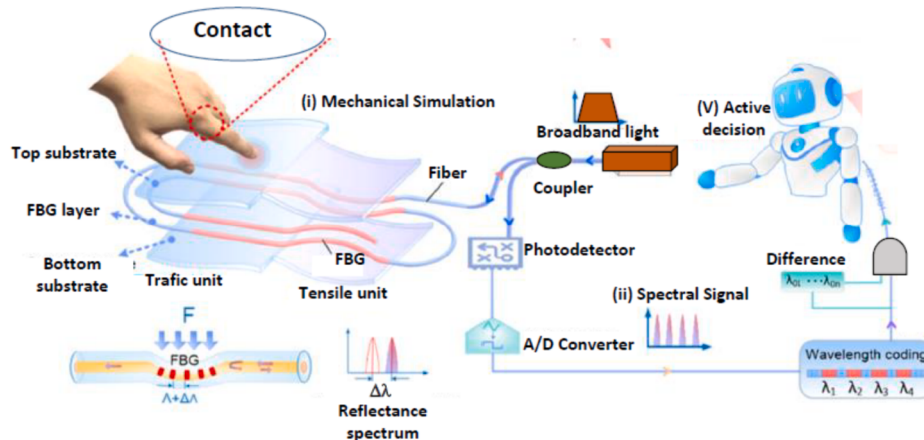


Fig. 11. FBG-base tactile sensor as suggested in [53].

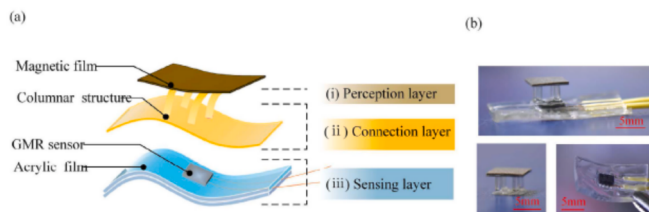


Fig. 12. Magnetic tactile sensor suggested in [66] (a) and its photograph (b).

2.6.3. Features of magnetic-based tactile sensors

Magnetic sensors have the advantage of featuring low hysteresis, robustness, and good repeatability. In addition, they are highly sensitive and can yield μN resolution if adequately shielded against EMI noise. They have been typically used for measuring low ranges of forces, not exceeding 5 N. In addition, their fabrication process is complex, as it requires precise magnetic particle injections and postprocessing at very high temperatures (e.g., up to 80 °C for 2 h in [66]), followed by magnetization. Another major drawback of these sensors is their steady loss of magnetization over time, which requires frequent calibration.

2.7. Discussions and prospects

From the above, it can be concluded that no sensing technique is currently available to accommodate all suitable attributes simultaneously: high sensitivity and spatial resolution, large area, immunity against EMI noise, low cost, high repeatability, ease of bend and stretch, and easy deployment. All the sensors are facing challenges preventing them from reaching the commercialization level. For instance, resistive and piezoresistive tactile sensors are flexible to bend and follow various desired shapes, which is highly required in tactile sensing applications. In addition, they need simple front-end electronics circuitry that may comprise a current source, amplifiers, and an analog-to-digital converter (ADC) chip, which can be easily integrated into an IoT (Internet of Things) device. However, they have the disadvantage of not being stretchable and featuring non-uniform conductivity distribution, which hinders their practicability. Very recently, in [67], this effect on the force range, sensitivity, and spatial resolution was investigated. The authors revealed that a conductivity of the detector of around 0.2 S/m could provide good performance with a force range of several Newtons. These disadvantages are not featured in capacitive tactile sensors, which, however, require complex circuitry to read capacitances of nF order and feature a prolonged data acquisition rate. Multimodality sensing can be a good alternative to using the complementary features of sensors simultaneously. This was considered in [68], where a multimodality tactile sensor simultaneously uses EIT and acoustic (piezoelectric) tomography for biomimetic robotic skin application. A hybrid hydrogel-elastomer material was used to build a skin-inspired tactile sensor, and arrays of electrodes and microphones were used for the EIT and acoustic sensing systems, respectively. A DNN algorithm was used to perform 2D image reconstruction. Also, piezoresistive-based tactile sensors, which typically provide contour information of objects, were combined with other sensors, such as piezoelectric sensors, to provide additional inner pressure information [41]. Further exploration of other similar multimodality tactile sensing would contribute to improving current tactile sensors. Table 2 lists some of the most recent works that used resistive, piezoresistive, capacitance, and FBG sensing techniques for tactile applications. It can be concluded that the spatial resolution of the resistive and piezoresistive sensors is relatively lower and that their localization and force measurement accuracy still need improvement. The other observation is that most systems use general-purpose computers for data processing, which hinders their real-time performance and portability. Finally, it can be observed that the works have yet to assess the effect of temperature variations on both resistive and piezoresistive tactile sensors and, to a lower extent, capacitance,

piezoelectric, and magnetic sensors, which can induce substantial conductivity changes. FBG sensors offer a great advantage of scalability, provided the sensitivity issue is sorted out. Another opportunity is to take advantage of the progress of AI edge and IoT devices to handle real-time object detection and classification using low-cost and portable hardware. For instance, nowadays, edge GPUs can offer a few TOPS/Watts on a small footprint [69]. In the 1990 s, machine vision was used to recognize human postures by placing multicolor markers on the body of interest and using dedicated 3D imaging systems [70] for their real-time tracking. Some systems could achieve real-time performance; however, the spatial resolution was poor as only a few markers were considered due to the high computation complexity of handling several of them. This issue can be easily overcome with the availability of powerful edge processors dedicated to AI acceleration. However, occlusions and adaptability to handle complex motion must also be tackled [71]. In [72], a fusion of visual and tactile sensing was suggested to enhance the recognition accuracy of objects with the exact visual representation but different tactile characteristics (e.g., roughness and friction). This capability, which is required in many industrial applications, is featured by human beings. A resistive sensor made of a polymer film with only one pair of electrodes connected to a Wheatstone bridge, followed by an amplifier and STM32f103C8T6 microcontroller, was used in the experiment to collect tactile information. The low number of electrodes used would hinder the accuracy of tactile sensing when multiple contact scenarios are required. The authors claim an accuracy of 96.6 %, outperforming all similar works. In another similar work [73], authors have shown that by fusing visual and tactile sensing (GelSight sensor) on 12 everyday objects, the prediction accuracy increases to 94 % compared to 80 % when using visual sensing alone. A desirable recent similar system was suggested in [7] (Fig. 13). The device includes a miniaturized visible light binocular camera (1920×1028 pixels @ 30 frames/s) incorporated in the tactile sensor itself together with a lighting system composed of 20 flexible white LEDs. A flexible $47 \times 47 \text{ mm}^2$ elastomer layer comprising dense coded markers is placed on the camera's top. The systems explore the relative motion of markers to predict the 3D object being gripped. Despite its complexity, using the coded marker rather than a highly dense marker, which reached up to 82 markers/cm^2 in [74] (e.g., using inkjet technology and silver ink) yields higher accuracy. In contrast, an XYZ RMSE error of less than 0.6 mm and 1 mm was claimed for non-occlusion and occlusion scenarios, respectively. Marker coding was done offline using Hamming distance by introducing a similarity penalty between local matrices representing the markers. While this technology offers the great advantage of not being influenced by EMI noises, it can be simplified using a single monocular camera. Another room for improvement of the sensor is to increase the number of markers, which was limited to 64×64 markers in this paper, and to mitigate the resistance of the flexible fabric against deformation caused by the target objects, especially in case of deeper contacts [75]. Commercially available sensors using similar concepts are already available and even associated with large datasets to build CNN models. This includes the compact $18.6 \times 14.3 \text{ mm}^2$ GelSight sensor, which features an impressive 8 MP to yield 1 mm accuracy in all three directions @ 25 frames/second [75,76]. The sensor was successfully used to accurately sense the texture and shape of real-life objects such as spheres and cuboids, but it can't be deployed to sense large objects that exceed finger size.

Measuring lateral strains or shear forces in addition to the regular forces is also being tackled by researchers. UpToDate, only capacitive tactile sensors were used, but researchers are also extending the approach to piezoresistive elements [29]. Liquid-based sensors offer a golden opportunity to trade between anthropomorphic shapes, sizes, and responses, provided that the SNR, leak, and non-linear response issues will be sorted out [77]. This sensing technology also requires multidisciplinary fluid mechanics and electronics skills, challenging its near-term realization. The magnetic field variations function of the strain can also be explored further using magnetic inductance

Table 2

List of some tactile sensors using different technologies.

Sensor & Common features	Work	Sensor [Area/number of electrodes/taxels]	Electronics	Observations [Image reconstruction latency-throughput/accuracy/resolution/sensitivity/power consumption]
Resistive sensors (+) easy to fabricate and low cost. Can handle large areas. Lower latency than capacitive sensors (-) prone to EMI noise. Yield low resolution. Weak repeatability in manufacturing. Consume higher power than capacitance and piezoelectric sensors	[92]	20 × 20 cm ² comprising 9 × 9 independent patches of 7 × 7 cm ² area	FPGA for control and PC for image reconstruction	64 ms/MSE error was 4.88 ± 1.63 mm
	[93]	A conductive polymer composite (CPC) material sandwiched between two sets of 32 orthogonal electrodes.	ARM Cortex M7 microcontroller controls the channel selection and the ADC conversion sequences.	100 frames/second 26 different objects/accuracy = 77.84 %/a maximal power consumption of 505 mW.
Piezoresistive sensor (+) easy to fabricate and low cost. Can handle large areas. Lower latency than capacitive sensors. They are used in object recognition. It can be integrated into a small area. (-) prone to EMI noise. Weak repeatability in manufacturing. Consume higher power than capacitance and piezoelectric sensors	[91]	54 × 54 cm ² sensor with 28 electrodes	Current source for excitation and a dedicated ERT system handling 28 electrodes. Use OC computer for image reconstruction.	30 ms/Average error = 77.4 mm, representing 17.2 % of the sensor width/force error was around 13 %.
	[34]	Four layers: one piezoresistive layer surrounded by two highly conductive layers (54 patches).	Used a variable voltage source. The selection of channels was done manually to provide the voltage to a PC through a DAQ card.	Weak repeatability of the sensor to respond to a constant strain of 10 kPa where a voltage variation of up to 4 % was observed
	[35]	The 16 × 16 pixels image is structured into five layers.	The front-end electronics of the system are based on an Arduino board (Mega2560 version), and the data processing and DCNN were implemented on a PC.	Accuracy = 92.73 %./Automatically recognize 13 objects of different shapes and weights based on tactile sensing
	[39]	200 × 200 mm ² using 16 electrodes	ADC5940 signal generator (0 to 200 kHz sinusoidal signal) and 16 to 1 ADG706 multiplexer controlled using STM32 microcontroller. A 4-wire impedance analyzer was used to determine the impedance changes. Image reconstruction was done using a PC	Experimental work was done on only one single strain contact for different strain intensities; however, this concept is worth exploring further as the fabrication process is simple and quick.
Capacitive sensor (+) Stretchable. Can measure shear forces. Adequate for small areas (fingertip). Consumes lower power than resistive and piezoresistive sensors. (-) prone to EMI noise. Yield high data acquisition latency. Weak repeatability in manufacturing.	[47]	2 × 2 sensor	a single chip with 24 bits of capacitance to a digital converter (CDC), AD7746 (from Analog Devices).	100 ms latency/ Its use of the hundreds of capacitances required in a reasonably sized tactile sensor is impractical.
	[50]	7 × 7 sensor.	Complex electronics to handle readings in the ff order	Up to 70 % Stretchable sensors. It can detect both static and dynamic pressures.
	[51]	2 × 2 sensor	no electronics was built as the assessment was done using only a commercially available LCR meter (LCR-821, GWINSTEK) to measure the capacitance at 100 kHz and 1 V excitation	A low hysteresis of 3.5 %, a normal sensitivity of 0.33 N ⁻¹ , and a tangential sensitivity of 0.091 N ⁻¹
	[52]	8 capacitive sensing elements tactile sensor targeting robotic finger	The measurement unit determines the In-phase quadrature (IQ) variable, providing the signals' amplitude and phase under an 81 kHz excitation.	400 Hz update rate/ a resolution of 50 ff to measure the strain intensity ranging from 1 to 16 N.
Optical sensors (+) immune to EMI noise. Easily scalable. (-) Low sensitivity to stress. Need temperature compensation circuitry. Can't be bended	[25]	A one-pixel, 20 mm diameter optical sensor	An FBG integrator connected to a PC	Sensor sensitivity < 0.087 N ⁻¹ with a standard deviation of 0.0219. No accuracy assessment was conducted. 92.4 % accuracy
	[38]	3 × 2 contacts using four brad sensors mounted on a 8 × 8 mm ² area		
	[31]	Four sensing units, separated by 4 mm. 3D-printed FBG tactile sensor targeting nursing robot		Sensitivity of 225.038/N and a response time to step excitation of 2 ms, with 32.93 dB SNR. The percentage error was less than 4.4 %.
	[72]	A 0.4 mm thick resistive sensor made of a polymer film with only one pair of electrodes.	The electrodes are connected to a Wheatstone bridge, followed by an amplifier and an STM32F103C8T6 microcontroller, yielding a 10 ms response time.	An accuracy of 96.6 %, outperforming all other similar works.
Visual + Resistive sensing (+) high spatial resolution. High image resolution. Yield visual + tactile information. (-) difficult deployment. Higher cost. Can't handle large areas.		47 × 47 mm ² sensor dopped with dense coded markers	A miniaturized visible light binocular camera (1920 × 1028 pixels @ 30 frames/s) is incorporated in the tactile sensor and a lighting system composed of 20 flexible white LEDs.	0.6 mm and 1 mm spatial resolution were claimed for non-occlusion and occlusion scenarios, respectively. The technology can be further simplified by using one single monocular camera.
Binocular cameras (+) high spatial resolution. High image resolution (-) difficult deployment. Can't handle large areas. Do not yield tactile information.				

tomography (MIT) [78].

Ensuring the scalability of the sensor is one of the challenges sought to be tackled to cover a large area with high spatial resolution. Besides the wiring, which induces electromagnetic interference noises, the readout speed is also another issue as a readout is usually done serially, in a time multiplexed manner [79]. High-speed electronics [80], intelligent subsampling [81], and data compression [82] were used to speed

up the acquisition time, which, however, could be more adequate for covering thousands of order sensors. An event-based technique, which mimics biological mechanoreceptors, is another alternative, as a signal is transmitted only when the associated sensor detects an event [83].

Table 3 lists most of the very recent piezoelectric-based tactile sensor chips, along with their respective spatial resolution and power consumption. As was mentioned earlier, these sensors are highly sensitive

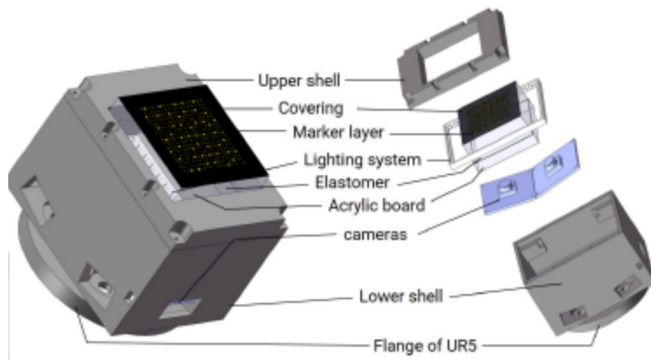


Fig. 13. Camera-based tactile sensor as suggested in [74].

making them suitable to be used in precise robotics. However, they are bandwidth-limited and thus, they may not satisfy the requirements of highly real-time robotic grasping systems.

3. Tactile sensor Algorithms

As was mentioned earlier, tactile sensing algorithms can be mainly categorized into ET, CNN, ANN, or a combination of any of them.

3.1. Non-AI algorithms for tactile sensing

Algorithms et al. offer the possibility of reconstructing the 2D image of the strain contacts using a relatively small number of electrodes, which is highly needed in tactile sensing applications as it will reduce the wirings and the weight of the device. Et al. algorithms can be either linear (e.g., linear-back propagation, LBP algorithm) or nonlinear (e.g., iterative Landweber, Gauss-Newton, and Tikhonov algorithms). They first run a forward model from which a sensitivity (Jacobian) matrix is derived. This matrix and the measurement data are then used for reconstruction in the inverse procedure. Linear algorithms have the advantage of having lower computational demand compared to nonlinear algorithms but yield lower image reconstruction accuracy. This has led researchers to mainly use non-linear algorithms with sometimes dedicated hardware accelerators. For instance, in [84], authors suggested using various nonlinear ET al algorithms using Landweber and Tikhonov algorithms. The associated tactile sensor was based on flexible skin composed of soft channels filled with fluid. The authors claim that both algorithms achieve very good accuracy but slightly lower than other AI-based algorithms (i.e., Radial Basis Function Neural Network, RBNN, and CNN). Other researchers commonly confirm this trend. In addition, ET algorithms are usually designed to yield only binary images and hence can only provide the location of the strains, not their respective intensity. In other words, piezoresistive tactile sensors are costly to host ET algorithms alone. This is why some researchers have recently suggested using ET and CNN/ANN simultaneously to enhance

the localization accuracy and estimate the strain's intensity. This also has the merit of reducing the computation time.

3.2. AI Algorithms for tactile sensing

In [85], a typical ANN algorithm was used to solve the inverse problem for EIT-based tactile sensing. Nevertheless, the work is only preliminary and limited to determining simple touch sensing. In another work [86], a deep learning algorithm was used as post-image processing to improve the image quality of EIT-based tactile sensors. The system could only detect two-point touch. Similarly, in [87], a machine learning-based combined with an EIT model was suggested to enhance the accuracy of object recognition of primitive objects (e.g., rectangles, circles, and triangles) for tactile sensing. However, again, the system could only determine the binary strain distribution, not its intensity. In another recent work [29], a CNN model for enhancing the EIT algorithm's accuracy and computation speed targeting tactile sensing was suggested. The model was trained for several scenarios using simulated data captured from finite element (FEM) simulation using EIDORS software. A spatial sensitivity-aware mean-squared error (SSA-MSE) loss function, which uses the sensor's intrinsic spatial sensitivity, was proposed to guarantee a well-posed EIT operation. The model comprises three fully connected layers of $4n^2$, n^2 , and n^2 neurons, respectively. Even though the algorithm has low computation time compared to the nonlinear EIT algorithms, the authors recognize that further optimization is needed to handle real-time applications like robotics. The algorithm was compared with several representative conventional methods: one-step GN as a linear method, iterative GN, primal-dual interior-point method (PDIPM), and structure-aware sparse Bayesian learning (SA-SBL) as nonlinear methods. The visual comparisons provided insights into each technique's performance and accuracy in capturing the reference image's conductivity variations. Similarly, in [39], the authors suggested another EIT-CNN model that has the potential to detect touch strength and force load by lowering the recognition of artifacts and noises. The sensing system uses a customized 16-electrode data acquisition circuit with an off-the-shelf impedance measurement chip AD5940. The model, which was designed in such a way as to avoid fully connected layers, uses architecture with a pre-reconstructor network to generate a pre-reconstructed image using an ET algorithm. This is followed by three convolutional layers and two deconvolutional layers for feature extraction and image reconstruction. The filter size and stride for all convolutional and deconvolutional layers are 3x3 and 1, respectively.

The activation function is the rectified linear unit (ReLU) function, and the Mean Squared Error (MSE) is the loss function. The Keras framework with a TensorFlow backend was used to build the EIT-CNN model, with 90 % of the total datasets used for training and 10 % for validation. The algorithm's performance was evaluated using two criteria: position error (PE), which assesses the accuracy of the touch position, and Mean Intersection over Union (MIOU), which measures the difference between the regions of the natural touch position and the reconstructed impedance distribution. The algorithm performed better

Table 3
Some recent piezoresistive and piezoelectric chips for tactile sensing.

Sensors	SCI, Robot[43] Piezoresistive	TBCAS[40] Piezoresistive	Sensors[44] Piezoresistive	JNN[45] MEMS	FingerPrint[42] Piezoelectric
# of sensors	80	6	9	4	192
Spatial resolution	> 1 mm	1 mm	2.5 mm	—	0.2 mm
Power Consumption	560 mW	—	—	42 mW	5.09 mW
Supply	3.3 V	3.3 V	—	5 V	5 V
Sensor data	spikes	spikes	spikes	spikes	spikes
ADC resolution	10 bits	12 bits	10 bits	24 bits	4 bits
Acquisition Datarate	8 MHz	21.6 kHz	130 kHz	146 kHz	<2.235 kHz
Classifier	KNN, MPL	ELM	SVM	SNN+KNN	SNN=Linear SVM
Preprocessing	ISI	None	ISI	None	None
Classification accuracy	88 %	92 %	97.12	94.2 %	99.166 %

reconstruction than traditional linearized imaging, especially when the SNR approached 40 dB. However, only one strain point was assessed experimentally, and no accuracy figures were mentioned. The training accuracy was below 0.1 %, and 10 % of the dataset was used for validation. In [39], a robust Spatial-temporal gradient algorithm, namely GradTac, was designed for tactile sensing applications, particularly emphasizing its implementation on bio-inspired sensors based on fluid motion-induced strains. The system uses a UR-10 manipulator with a Shadow Dexterous Hand to capture 24 taxel readings at 100 Hz. The GradTac algorithm incorporates a sophisticated ANN with seven hidden layers featuring widths of 8, 16, 32, 64, 32, 16, and 8, respectively. Employing the L2 loss function during training, the network excels at computing a regression curve, effectively mapping forces to contour areas. Including a logistic activation function and an inversely scaled learning rate further refine its performance. Training over 5,000 epochs on 200 data points, the algorithm establishes a robust foundation for force-contour correlation: A mean absolute percentage error of less than 0.78 % was obtained for different shapes that include circle and diagonal, horizontal, and vertical lines strains. GradTac contrasts its neural network approach with two alternative regression methods in a comprehensive comparative analysis. The first employs stochastic gradient descent regression with ElasticNet regularization and log loss, while the second adopts L2 regularized regression with Huber loss. The mean absolute percentage error (MAP) is a metric for this comparison, highlighting GradTac's commitment to evaluating its algorithm against diverse methodologies to pursue tactile sensing excellence. Among the works that have solely used CNN, one can cite the piezoresistive tactile sensor targeted for humanoid robot applications [35]. The associated algorithm employs transfer learning with 19 different CNN models augmented with a multimodal optimization technique. The sensor was trained by capturing randomly positioned objects of 19 classes, compiling a substantial dataset. Experimental results have shown that the InceptionResNetV2 CNN model provided superior performance with 91.82 % accuracy. However, using the multimodal learning method that included InceptionResNetV2 and XceptionNet, the highest recognition rate of 92.73 % was achieved. More recently, in [30], a dataset, including 3600 samples (100 samples per material) for 36 everyday household materials, was compiled. The authors proposed a TactNet-II network based on TactNet [77] and reached an accuracy for the material classification task as high as 95.0 % utilizing tactile data only. Table 4 shows a non-exhaustive list of the most recent algorithms used in tactile sensing. The trend is to move away from traditional signal processing and pattern recognition algorithms (e.g., Haar wavelet transform [68] and Kernel principal analysis (PCA) in [69]) and use rather ET, CNN, ANN, or a combination of a few of them. The accuracy for strain localization is generally high and exceeds 90 %. However, only a few classes could be handled (22 classes in [65]). Also, while the ET-CNN and solely CNN algorithms achieve the best performance, only a few classes have been handled so far (i.e., 22 classes in [22]). Also, most of the algorithms were hosted on a PC. With the availability of very computation-powerful and energy-efficient GPU and FPGA hardware accelerators, portable and real-time implementation of these algorithms can be achieved. This is particularly the case for combined visual-tactile sensing, where various types of CNN algorithms have been suggested [75]. Very recently, transformer AI, which leverages tactile and visual sensing, was suggested for the robotic grasping of deformable objects such as fruits [96]. Compared to the CNN-LSTM network, the algorithm performs better in accuracy (up to 3.1 % accuracy increase for slip measurement) and computation speed. These results are associated with different experimental setups done on fruit grasping.

4. Conclusion

Several tactile sensors have been suggested in the literature. Despite the significant improvements made so far, efforts are still required to improve their execution time, accuracy, range, sensitivity,

Table 4
List of some recent tactile sensing algorithms.

Algorithm	Work	Algorithm Description	Observations
EIT-ANN	[85]	Use ANN to solve the inverse problem	the work is at only a preliminary stage and is limited to determining simple touch-sensing
EIT-CNN	[39]	EIT for image reconstruction followed by a CNN model (three convolutional layers and two deconvolutional layers) for feature extraction and image reconstruction)	Better performance than traditional linearized imaging algorithms, especially when the SNR approaches 40 dB. However, only one strain point was assessed experimentally, and no accuracy figures were mentioned.
EIT-CNN	[29]	EIT for image reconstruction followed by a CNN model for feature extraction and image reconstruction. Used SSA-MSE loss function	Better accuracy than one-step GN and iterative GN algorithms. The system could not achieve real-time performance (e.g., 64 ms latency)
Spatial-temporal gradient algorithm	[39]	converts discrete data points from spatial tactile sensors into spatiotemporal surfaces and tracks tactile contours across these surfaces	A mean absolute percentage error of less than 0.78 % was obtained for different shapes that include circle as well as diagonal, horizontal, and vertical lines strain
Multimodal CNN	[35]	Used 19 different CNN models augmented with a multimodal optimization technique	InceptionResNetV2 CNN model provided superior performance with 91.82 % accuracy. However, using the multimodal learning method that included InceptionResNetV2 and XceptionNet, the highest recognition rate of 92.73 % was achieved. (20 classes)
RestNet-DCNN	[88]	DCNN	28 × 59 pixels piezoresistive sensor to achieve 95.36 % accuracy (22 classes)
AlexNet-DCNN	[89]	DCNN	28 × 59 pixels piezoresistive sensor to achieve 91.6 % accuracy (8 classes)
AlexNet-DCNN	[90]	DCNN	768 pixels piezoresistive sensor to achieve 91.6 % accuracy (2 classes)
TactNet-II	[30]	The model is based on TactNet	A dataset, including 3600 samples (100 samples per material) for 36 everyday household materials. The accuracy of the material classification task was as high as 95.0 %, utilizing only tactile data.
k-nearest neighbor (KNN), support vector machines (SVMs), and MLP	[75]	Unlike Siamese networks that learn similarities or differences between pairs of data points, triplet networks use three input samples (anchor, positive, and negative) to learn embeddings that encode the similarity information between them.	A gelsight tactile sensor was used. An impressive 200 different objects were considered (20 samples per object) to achieve an accuracy of up to 77.78 %.

manufacturability, and low cost. None of the current techniques can simultaneously fulfill these features, such as combining visual and tactile sensing, allowing multimodality sensing to be considered. One way to categorize tactile sensors is their coverage scale, which is usually inversely proportional to the spatial resolution. While capacitance, piezoelectric, and visual-tactile sensors are typically used for small tactile areas, piezoresistive and resistive sensors are generally used to be deployed for larger areas. In the near term, resistive and piezoresistive sensors are the most promising, especially if issues such as uniform electrical conductivity distribution stretchability of the material and temperature compensation issues are sorted out. The associated front-end analog electronics and digital hardware accelerators are readily available as they are very similar to the ones required in ET systems. This would also give the opportunity to camera-based tactile sensors using dense marker distribution, which has the advantage of being contactless and does not require specific material fabrication. Nevertheless, it yields a higher resolution than a human being. For the longer term, miniaturization of the optical fiber interrogator would make FBG-based tactile sensing very promising. These sensors are the only ones with the advantage of not being sensitive to electromagnetic interference noise, which constitutes an obstacle to increasing the resolution and the size of the tactile sensors. They yield the additional advantage of yielding distributed sensing. Nevertheless, they suffer from low sensitivity, especially if the distance between grating elements is small. In addition, they can't cope with bending deformation, significantly restricting their application domain. Furthermore, they require cumbersome FBG integrator circuitry, which is not easily portable and costly. Another challenge not addressed in the literature is the requirement to measure temperature variations at every grating point, which is practically impossible. This list of challenges has made tactile-based sensing technology not commercially available. On the other hand, resistive and piezoresistive tactile sensors are flexible to bend and follow various desired shapes, which is highly required in tactile sensing applications. In addition, they require simple front-end electronics circuitry that may comprise a current source, amplifiers, and an analog-to-digital converter (ADC) chip, which can be easily integrated into an IoT (Internet of Things) device. However, they have the disadvantage of not being stretchable and featuring non-uniform conductivity distribution, which hinders their practicability. This has motivated researchers to consider using multimodality tactile sensing, such as combining resistive and acoustic (piezoresistive) techniques. The success of capacitive-based sensors, which feature the best stretchability, would depend on the availability of quick and accurate capacitive measurement systems. In addition, the sensors themselves need to be protected against eventual EMI, which was not tackled in the literature. In summary, all existing tactile sensors still need help to prevent them from being commercially available, at least on a large scale. Compact and low power consumption hardware accelerators based on GPU or FPGA are readily available to host measurement and imaging algorithms based on AI or non-AI algorithms. The critical part remains the sensing part.

CRediT authorship contribution statement

Mahmoud Meribout: Validation, Supervision. **Natnael Abule Takele:** Methodology. **Olyad Derege:** Formal analysis. **Nidal Rifiki:** Resources. **Mohamed El Khalil:** Validation. **Varun Tiwari:** Writing – review & editing. **Jing Zhong:** Supervision.

Declaration of competing interest

The authors declare that they have no known competing financial interests or personal relationships that could have appeared to influence the work reported in this paper.

Data availability

No data was used for the research described in the article.

References

- [1] B.D. Argall, A.G. Billard, A survey of tactile human-robot interactions, *Rob. Auton. Syst.* 58 (10) (2010) 1159–1176.
- [2] M. Park, B.-G. Bok, J.-H. Ahn, M.-S. Kim, Recent advances in tactile sensing technology, *Micromachines* 9 (2018).
- [3] N. Gardella, S. Riggs, Establishing natural tactile mappings: Mapping tactile parameters to continuous data concepts, *IEEE Transactions on Haptics*, Early access, 2024.
- [4] H. Meng, et al., Design and application of flexible resistive tactile sensor, *IEEE Trans. Instrum. Meas.* 72 (2023) 304–314.
- [5] T.D. Nguyen, J.S. Lee, Recent development of flexible tactile sensors and their applications, *Sensors* 22 (1) (2022).
- [6] A. Adler and D. Holder, “Electrical impedance Tomography: Methods, history, and applications,” *Electrical Impedance Tomography: Methods, History, and Applications*, pp. 1–499, Dec. 2021.
- [7] M. Valle, Editorial of the special issue ‘tactile sensing technology and systems’, *Micromachines (Basel)* 11 (5) (2020).
- [8] J. Xu, J. Pan, T. Cui, S. Zhang, Y. Yang, and T. L. Ren, “Recent Progress of Tactile and Force Sensors for Human-Machine Interaction,” *Sensors* 2023, Vol. 23, Page 1868, vol. 23, no. 4, p. 1868, Feb. 2023.
- [9] X. Lu, et al., 3-D tactile-based object recognition for robot hands using force-sensitive and bend sensor arrays, *IEEE Trans. Cognit. Dev. Syst.* 15 (4) (2023) 505–515.
- [10] I. Andrussov, et al., Minsight: a fingertip-sized vision-based tactile sensor for robotic manipulation, *Adv. Intell. Syst.* 5 (8) (2023).
- [11] M. Costanzo, et al., Two-fingered in-hand object handling based on force/tactile feedback, *IEEE Trans. Rob.* 36 (1) (2020) 157–173.
- [12] G. Zhou, et al., Tactile gloves predict load weight during lifting with deep neural networks, *IEEE Sens. J.* 23 (16) (2023) 18798–18809.
- [13] Y. Li, et al., A machine learning-assisted multifunctional tactile sensor for smart prosthetics, *InfoMat* 5 (9) (2023) e12463.
- [14] M. Azechi, S. Okamoto, Bumps and Dents are not Perceptually Opposite When Exploring with Lateral Force Cues, *IEEE Transactions on Haptics*, Early Access, 2024.
- [15] M. Mir, et al., A minimally invasive robotic tissue palpation device, *IEEE Transactions on Biomedical Engineering*, Early Access, 2024.
- [16] Z. Sun, et al., “Augmented tactile-perception and haptic-feedback rings as human-machine interfaces aiming for immersive interactions,” *Nature Communications* 2022 13:1, vol. 13, no. 1, pp. 1–13, Sep. 2022.
- [17] M. Zhu, et al., Haptic-feedback smart glove as a creative human-machine interface (HMI) for virtual/augmented reality applications, *Sci. Adv.* 6 (19) (2020).
- [18] A. Schmitz, et al., Methods and technologies for the implementation of large-scale robot tactile sensors, *IEEE Trans. Rob.* 27 (3) (2011) 389–400.
- [19] J. Weichert, et al., Tactile sensing with scalable capacitive sensor arrays on flexible substrates, *J. Microelectromech. Syst.* 30 (6) (2021) 915–929.
- [20] D. H. Lee, et al., “Flexible piezoresistive tactile sensor based on polymeric nanocomposites with grid-type microstructure,” *Micromachines (Basel)*, vol. 12, no. 4, Apr. 2021.
- [21] W. Lin, B. Wang, G. Peng, Y. Shan, H. Hu, Z. Yang, Skin-inspired piezoelectric tactile sensor array with crosstalk-free row+column electrodes for spatiotemporally distinguishing diverse stimuli, *Adv. Sci.* 8 (3) (2021).
- [22] C. Tang, et al., A nonarray soft capacitive tactile sensor with simultaneous contact force and location measurement for intelligent robotic grippers, *IEEE Trans. Instrum. Meas.* 73 (2024) 73–83.
- [23] X. Duan, et al., “Artificial skin through the super-sensing method and electrical impedance data from conductive fabric with the aid of deep learning,” *Scientific Reports* 2019 9:1, vol. 9, no. 1, pp. 1–11, Jun. 2019.
- [24] W. Navaraj, et al., Fingerprint-enhanced capacitive-piezoelectric flexible sensing skin to discriminate static and dynamic tactile stimuli, *Adv. Intell. Syst.* 1 (7) (2019) 1900051, <https://doi.org/10.1002/AISY.201900051>.
- [25] Y. Liu, et al., An optical contact force sensor for tactile sensing based on specklegram detection from concatenated multimode fibers, *Opt. Laser Technol.* 143 (2021) 107362.
- [26] H. Yang, et al., Liquid Lens-Based Optical Tactile Sensor with a Touch-Sensing Separable Structure, *Adv Mater Interfaces*, 2022.
- [27] Y. Zhu, et al., Recent advances in resistive sensor technology for tactile perception: a review, *IEEE Sens. J.* 22 (16) (2022) 15635–15649.
- [28] C. Liu, Design of active sensing smart skin for incipient slip detection in robotics applications, *IEEE Trans. Mechatron.* 28 (3) (2023) 890–899.
- [29] H. Park, et al., Deep neural network based electrical impedance tomographic sensing methodology for large-area robotic tactile sensing, *IEEE Trans. Rob.* 37 (5) (2021) 1570–1583.
- [30] A. Tulbure and B. Bäuml, “Superhuman performance in tactile material classification and differentiation with a flexible pressure-sensitive skin,” in Proc. IEEE-RAS 18th Int. Conf. Humanoid Robots (Humanoids), Nov. 2018, pp. 1–9.
- [31] T. Li, et al., RSM-based data-driven optimized design of a 3-D-printed building block-type FBG tactile sensor for nursing robots, *IEEE Trans. Instrum. Meas.* 72 (2023) 1–12.

- [32] H. Wu, et al., "New Flexible Tactile Sensor Based on Electrical Impedance Tomography," *Micromachines (Basel)*, vol. 13, no. 2, Feb. 2022, doi: 10.3390/MI13020185.
- [33] W. Matusik et al., "Wearable glove with hybrid resistive pressure sensors," US Patent# 11,625,096 B2, April 11, 2023.
- [34] G. H. Büscher et al., "Flexible and stretchable fabric-based tactile sensor," *Rob Auton Syst*, vol. 63, no. P3, pp. 244–252, Jan. 2015.
- [35] S. Pohtongkam, J. Srinonchat, Tactile object recognition for humanoid robots using new designed piezoresistive tactile sensor and dcnn, *Sensors* 21 (18) (2021) Sep, <https://doi.org/10.3390/S21186024>.
- [36] T. Sagisaka, et al., High-density conformable tactile sensing glove, in: In IEEE-RAS International Conference on Humanoid Robots (Humanoids, 2011, pp. 537–542.
- [37] T. Mouri, Kawasaki, Humanoid robot hand and its applied research, *J. Rob. Mechatronics* 31 (1) (2019) 16–26, <https://doi.org/10.20965/jrm.2019.p0016>.
- [38] G. Schwartz , B. C. Tee , J. Mei , A. L. Appleton , H. Kim do, H. Wang, Z. Bao, *Nat. Commun.* 2013, 4, 1859.
- [39] H. Chen et al., "A convolutional neural network based electrical impedance tomography method for skin-like hydrogel sensing," 2022 IEEE International Conference on Robotics and Biomimetics, ROBIO 2022, pp. 178–183, 2022.
- [40] W. Lee et al., "A neuro-inspired artificial peripheral nervous system for scalable electronic skins", *Sci.Robot.*, Vol. 4, NO 32, 2019.
- [41] X. Lu et al., "3-D Tactile-Based Object Recognition for Robot Hands Using Force-Sensitive and Bend Sensor Arrays", *IEEE Transactions on Cognitive and Developmental Systems*, Vol. 15, no. 4, 2023.
- [42] M. Alea et al., "A Fingertip-Mimicking 12×16 200μm-Resolution e-skin Taxel Readout Chip with per-Taxel Spiking Readout and Embedded Receptive Field Processing", *IEEE Transactions on Biomedical Circuits and Systems*, pp. 1-12, April 2024.
- [43] C. Bartolozzi, et al., Robots with a sense of touch, *Nature* 15 (9) (2016) 921–925.
- [44] M. Rasouli, et al., An extreme learning machine-based neuromorphic tactile sensing system for texture recognition, *TBCAS* (2018).
- [45] M. Alea, et al., Power-efficient and accurate texture sensing using spiking readouts for high-density e-skins, *BioCAS* (2022).
- [46] N. Nikafrooz, Z. Fuge, A. Leonessa, Grasp control of a cable-driven robotic hand using a PVDF slip detection sensor, *ArXiv*. (2022).
- [47] S.C. Mansfeld, B.C. Tee, R.M. Stoltenberg, C.V. Chen, S. Barman, B.V. Muir, A. N. Sokolov, C. Reese, Z. Bao, *Nat. Mater.* 9 (2010) 859.
- [48] B.C. Tee, C. Wang, R. Allen, Z. Bao, *Nat. Nanotechnol.* 7 (2012) 825.
- [49] C. Pan, L. Dong, G. Zhu, S. Niu, R. Yu, Q. Yang, Y. Liu, Z.L. Wang, *Nat. Photonics* 7 (2013) 752.
- [50] X. Zhao, et al., Flexible, stretchable and wearable multifunctional sensor array as artificial electronic skin for static and dynamic strain mapping, *Adv. Electron. Mater.* 1 (7) (2015).
- [51] W. Gong, J. Lian, Y. Zhu, Capacitive flexible haptic sensor based on micro-cylindrical structure dielectric layer and its decoupling study, *Measurement* 223 (2023) 113785.
- [52] M. Al Shawabkeh, et al., Highly stretchable additively manufactured capacitive proximity and tactile sensors for soft robotic systems, *IEEE Trans. Instrum. Meas.* 72 (2023) 1–12.
- [53] J. Cheng et al., "A four-capacitor tactile sensor based on bump structure and compensating method to reduce inertial interference for robotic tactile sensing," *IEEE Sens J*, Sep. 2023.
- [54] T. Li, et al., Fault-tolerant six-axis FBG force/moment sensing for robotic interventions, *IEEE Trans. Mechatron.* 28 (6) (2023) 3537–3550.
- [55] K. Takashima, K. Ota, M. Yamamoto, M. Takenaka, S. Horie, K. Ishida, Development of catheter-type tactile sensor composed of polyvinylidene fluoride (PVDF) film, *ROBOMECH J*, 6 (1) (2019) 1–11.
- [56] U. Kim, Y.B. Kim, D.-Y. Seok, J. So, H.R. Choi, A surgical palpation probe with 6-axis force/torque sensing capability for minimally invasive surgery, *IEEE Trans—Ind Electron.* 65 (3) (2018) 2755–2765.
- [57] T. Li, et al., A surgical palpation probe with 6-axis force/torque sensing capability for minimally invasive surgery, *IEEE Trans. Instrum. Meas.* 72 (2023) 4006513–4006521.
- [58] M. Luca, S. Emiliano, M. Carlo, S. Paola, M. Arianna, S. Edoardo, M.O. Calogero, *Soft Rob.* 7 (2020) 409.
- [59] J. Man, G. Chen, J. Chen, Recent progress of biomimetic tactile sensing technology based on magnetic sensors, *Biosensors* 12 (11) (2022) 1054.
- [60] Q. Zhou, B. Ji, F. Hu, J. Luo, B. Zhou, Magnetized micropillar-enabled wearable sensors for touchless and intelligent information communication, *Nano-Micro Lett.* 13 (1) (2021) 197.
- [61] J.K. Ruffalo, J.D. Miller, C.J. Berkland, Compression sensors constructed from ferromagnetic particles embedded within soft materials, *MRS Commun.* 11 (2) (2021) 94–99.
- [62] L. Jamone, L. Natale, G. Metta, G. Sandini, Highly sensitive soft tactile sensors for an anthropomorphic robotic hand, *IEEE Sens. J.* 15 (8) (2015) 4226–4233.
- [63] H. Wang, et al., Design methodology for magnetic field-based soft triaxis tactile sensors, *Sensors* 16 (9) (2016) 1356.
- [64] A. Alfadhel, M. A. Khan, S. Cardoso, and J. Kosel, "A single magnetic nanocomposite cilia force sensor," in Proc. IEEE Sensors Appl. Symp. (SAS), Apr. 2016, pp. 1–4.
- [65] M. Neto, P. Ribeiro, R. Nunes, L. Jamone, A. Bernardino, S. Cardoso, A soft tactile sensor based on magnetics and hybrid flexiblerigid electronics, *Sensors* 21 (15) (2021) 5098.
- [66] Li, et al., A tactile sensor based on magnetic sensing: design and mechanism, *IEEE Trans. Instrum. Meas.* (2024).
- [67] S. Yoshimoto, et al., Design of a high-performance tomographic tactile sensor by manipulating the detector conductivity, *IEEE Trans. Ind. Electron.* (2024) 1–12.
- [68] H. Park, et al., A biomimetic elastomeric robot skin using electrical impedance and acoustic tomography for tactile sensing, *Sci. Robot.* 8 (2022), <https://doi.org/10.1126/scirobotics.abm7187>.
- [69] V.K. Tiwari, M. Meribout, L. Khezzar, K. Alhammadi, M. Tarek, Electrical tomography hardware systems for real-time applications: a review, *IEEE Access* (2022) 357–367.
- [70] Eiichi Hosoya et al., "Real-time 3D Feature Extraction Hardware Algorithm with Feature Point Matching Capability". Machine Vision a& Application Conference, MVA'96, Tokyo, Japan: pp. 430-433, 1996.
- [71] Y. Zhang, Z. Kan, Y. Alexander Tse, Y. Yang, and M. Yu Wang, "FingerVision tactile sensor design and slip detection using convolutional LSTM network," 2018, arXiv: 1810.02653.
- [72] B. Li, et al., VITO-transformer: a visual-tactile fusion network for object recognition, *IEEE Trans. Instrum. Meas.* 72 (4) (2023).
- [73] H. Xue, et al., 3D dense reconstruction of vision-based tactile sensor with coded markers, *IEEE Trans. Instrum. Meas.* (2024).
- [74] Y. Yang, et al., Granularity-dependent roughness metric for tactile sensing assessment, *IEEE Trans. Instrum. Meas.* 72 (2023) 1–12.
- [75] URL: https://www.gelsight.com/wp-content/uploads/2023/01/GelSight_Datasheet_GSMini_12.20.22.pdf. Last visited on 12/4/2023.
- [76] K. Ganguly, et al., GradTac: spatio-temporal gradient based tactile sensing, *Front Robot AI* 9 (2022) 898075.
- [77] G. Dingley, et al., EM-Skin: an artificial robotic skin using magnetic inductance tomography, *IEEE Trans. Instrum. Meas.* 72 (2023) 1–12.
- [78] M.L. Dong, J. Zhang, A review of robotic grasp detection technology, *Robotica* (2023).
- [79] W. W. Lee, S. L. Lukreja, N. V. Thakor, A kilohertz kilotaxel tactile sensor array for investigating spatiotemporal features in neuromorphic touch, in Proceedings of the 2015 IEEE Biomedical Circuits and Systems Conference (BioCAS) (2023), pp. 1–4.
- [80] W. Fukui, F. Kobayashi, F. Kojima, H. Nakamoto, N. Imamura, T. Maeda, H. Shirasawa, High-speed tactile sensing for array-type tactile sensor and object manipulation based on tactile information, *J. Robot.* 2011 (2022) 691769.
- [81] O. Oballe-Peinado, J. A. Hidalgo-Lopez, J. A. Sanchez-Duran, J. Castellanos-Ramos, F. Vidal-Verdu, Architecture of a tactile sensor suite for artificial hands based on FPGAs, in Proceedings of the 4th IEEE RAS & EMBS International Conference on Biomedical Robotics and Biomechatronics (BioRob) (2021), pp. 112–117.
- [82] C. Bartolozzi, C. Bartolozzi, P. M. Ros, F. Diotallevi, N. Jamali, L. Natale, M. Crepaldi, D. Demarchi, Event-driven encoding of off-the-shelf tactile sensors for compression and latency optimization for robotic skin, in Proceedings of the 2017 IEEE/RSJ International Conference on Intelligent Robots and Systems (IROS) (2017), pp. 166–173.
- [83] K. Liu, et al., Biosens. *Bioelectrom. X* 10 (2022) 10016.
- [84] N. Biasi, N. Carbonaro, L. Arcarisi, A. Tognetti, Combining physics-based simulation and machine learning for eit-based tactile sensing, *IEEE Sens. 2020* (2020) 1–4.
- [85] X. Duan, et al., Artificial skin through supersensing method and electrical impedance data from conductive fabric with aid of deep learning, *Sci. Rep.* 9 (1) (2019) 1–11.
- [86] Z. Husain, N.A. Madjid, P. Liatsis, Tactile sensing using machine learning-driven electrical impedance tomography, *IEEE Sens. J.* 21 (10) (2021).
- [87] J.M. Gandarias, A. García-Cerezo, J.M. Gómez-de-Gabriel, CNN-based methods for object recognition with high-resolution tactile sensors, *IEEE Sens. J.* 19 (2019) 6872–6882.
- [88] Gandarias, et al, A. Human and object recognition with a high-resolution tactile sensor. In Proceedings of the 2017 IEEE SENSORS, Glasgow, UK, 29 October–1 November 2017.
- [89] Albinia, A.; Denei, S.; Cannata, G. Human hand recognition from robotic skin measurements in human-robot physical interactions. In Proceedings of the 2017 IEEE/RSJ International Conference on Intelligent Robots and Systems (IROS), Vancouver, BC, Canada, 24–28 September 2017.
- [90] H. Lee et al., "Predicting the Force Map of an ERT-Based Tactile Sensor Using Simulation and Deep Networks," *IEEE Transactions on Aut. Science and Engineering*, vol. 20, no. 1, pp. 425–439, Jan. 2023.
- [91] S. Russo, et al., EIT-based tactile sensing patches for rehabilitation and human-machine interaction, *Biosystems* 22 (2019) 13–17.
- [92] X. Wang, et al., Leveraging Tactile sensors for low latency embedded smart hands for prosthetic and robotic applications, *IEEE Trans. Instrum. Meas.* 72 (2023) 1–12.
- [93] Y. Han, et al., Learning generalizable vision-tactile robotic grasping strategy for deformable objects via transformer, *IEEE Trans. Mechatronics* (2024) 1–14.